Large emission enhancement and emergence of strong coupling with plasmons in nanoassemblies: Role of quantum interactions and finite emitter size

Riya Dutta,[1] Kritika Jain,[2] Murugesan Venkatapathi,[2,*] and J. K. Basu[1,†]
[1]*Department of Physics, Indian Institute of Science, Bangalore 560012, India*
[2]*Computational and Statistical Physics Laboratory, Indian Institute of Science, Bangalore 560012, India*

(Received 5 June 2019; revised manuscript received 29 September 2019; published 15 October 2019)

The Purcell effect has been the basis for several decades in understanding enhancement of photonic efficiency and decay rates of emitters through their coupling to cavity modes and metal nanostructures. However, it is not clear whether this regime of radiative enhancements can be extended to ultrasmall nanoparticle sizes or interparticle distances. Here we report large radiative enhancements of quantum dot assemblies with extremely small metal nanoparticles and emitter-particle separations R of a few nanometers, where Purcell effect would lead to either no enhancements or quenching. We invoke a new regime of radiative enhancements to explain the experimental data and also correctly predict the emergence of strong coupling below certain R, as observed in experiments. In addition, we show that the widely used point emitter approximations diverge from actual observations in the case of finite size emitters at such small separations.

DOI: 10.1103/PhysRevB.100.155413

I. INTRODUCTION

Next-generation photonic devices [1], optical quantum communication, and information processing [2] will rely on generating QE assemblies with high photonic efficiencies [3] that can be coupled to sources of localized radiation typically enabled by plasmons in ultrasmall metal nanoparticles (MNPs). Compact films of QEs like colloidal quantum dots (QDs) with high radiative photonic efficiency are a critical component in various display [2,4], light-emitting, and photonic devices [1], nanolasers [5,6], photovoltaic [7,8] and thermoelectric devices and photodetectors [9]. Coupled with high radiative photonic efficiency [3], achieving high spatial density in these assemblies and arrays not only allows for improved spatial resolution in display devices but also for emergence of interesting optoelectronic properties [10–12] in these materials. A widely used method to enhance QD decay rates is to couple them to plasmons in MNPs and templates [13–15]. The rate enhancements in all such cases can be well explained using the Purcell effect [16–18] which, in general, deals with the modified density of optical states due to cavity-emitter interactions [3,19–21]. While exploitation of this effect has been well demonstrated with larger MNPs (>50 nm in diameter) that scatter strongly, and at separations on the order of dimensions of the MNP, it is not clear whether it will be relevant for much smaller separations and with small MNP as would be necessary for the high-density QD films. Hence research on these systems will not only help in obtaining better future nanophotonic devices but also throw light on fundamental aspects of emitter-matter interactions at the nanoscale.

In the recent past, some observations by us [22–25] and others [26,27] have shown that the conventional local density of optical states defining the Purcell regime may not hold for extremely small MNPs (<10 nm in diameter). In actual experiments, the QEs have finite sizes which can become comparable to the separation from MNPs. Typical models of the Purcell effect involve the point emitter approximation, which could lead to the perceived divergence of the experimental results from the theoretical calculations. But to draw such conclusions here, one should thus take into account the finite size of the QDs. Hence, we also present evaluations that consider the QD as a multipole emitter [28] of a finite size.

Apart from finite size effects, the strength of coupling between quantum emitters (QEs) and MNPs in a multiparticle hybrid assembly play a significant role in determining their optical properties [29–31]. In the case of the uncoupled or the classical independent emitter approximation, one assumes no additional probability of emission due to the MNPs. But when one interprets the classically evaluated electromagnetic fields due to a neighboring emitter as probability amplitudes of a photon emitted, one can infer an increase in probability of decay due to its superposition with the scattered field from the MNPs [32]. This simple quantum superposition is satisfied by observations, and is a signature of the weak-coupling regime of emitter and matter (or a cavity) that is widely known as the Purcell regime. Recently, a theoretical approach to account for the modified absorption and emission due to strong coupling of an emitter with metals was reported [33] where such a simple superposition may not hold. This work accounted for the anomalous enhancements of emitters near extremely small fully absorbing MNPs and the unexpected large enhancements observed in surface enhanced Raman spectroscopy.

In this paper, we use compact monolayer colloidal QD films sparsely doped with tiny gold nanoparticles (AuNP) (D_M <4 nm) to demonstrate large radiative photonic enhancements

*murugesh@iisc.ac.in
†basu@iisc.ac.in

in emission from these films which varies in a nonmonotonic manner with QD-AuNP separation, R, between 1.5–5 nm. All conventional models of emitter-plasmon interactions, which only predict a quenching [30,34] of emission in this regime, fail to explain these observations. Detailed models which self-consistently incorporate the strong quantum coupling between QDs and AuNPs [35] can explain the experimental observations very satisfactorily. In addition, this model predicts emergence of strong coupling at small R regime of emitter-metal separations, with incorporation of the finite size of emitters, which is also confirmed in experiments. Our results thus suggest new directions in nanophotonics research involving emitter-matter interactions which go beyond the well-established Purcell regime in obtaining high-efficiency photonic devices, with possible implications for related optoelectronic as well as photodetector [9] and photovoltaic devices [7]. Further, fundamental insights on importance of quantum interactions and the emitter's finite size in nanophotonics of hybrid nanoassemblies emerges from our work.

II. EXPERIMENTAL METHODS

The experimental system demonstrated here is based on hybrid films formed by AuNPs of mean diameter (D_M) 3.8 nm and cadmium selenide (CdSe)-zinc sulphide (ZnS) graded coreshell colloidal QDs of average diameter (D_E) 6.7 nm, prepared using the well-known Langmuir-Blodgett method [23,24]. Here AuNPs are used as a plasmonic material, doped in these QD monolayers at a particular ratio. While keeping the ratio of AuNPs to QD fixed, the surface separation between nanoparticles, R, is varied by controlling both the organic capping around the respective AuNPs and QDs or by varying areal density of the corresponding Langmuir monolayers. Photoluminescence (PL) measurements of the samples were implemented using a WiTec alpha SNOM setup in confocal mode [23]. A 488-nm argon (Ar) laser is used as an excitation source for PL measurements. Time-resolved photoluminescence (TRPL) measurements were performed with the PicoQuant-MicroTime 200 fluorescence lifetime microscope system. We used a laser source of repetition rate 2 MHz to ensure full decay of QDs. All measurements were performed in ambient condition.

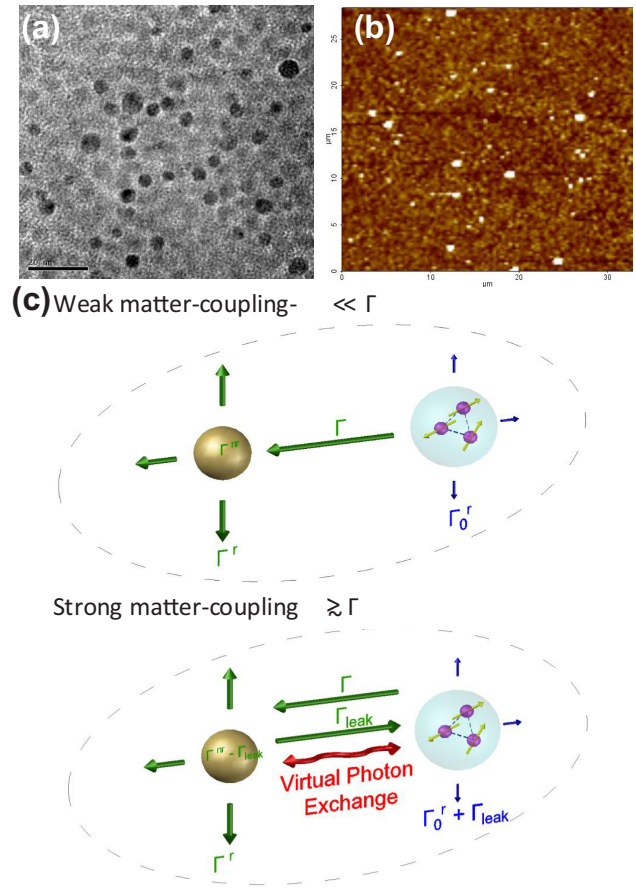

FIG. 1. (a) TEM images of QD-AuNP monolayer film. Dark features represent AuNPs. (b) AFM scanning image represents the packed arrangement of AuNP and QDs. (c) Interactions and components of decay in the model; Γ_0^r and Γ represent the decay of independent QE and AuNP, and Γ_{leak} is due to strong coupling with the AuNP, respectively. The golden sphere represents the metal nanoparticle (AuNP) which was modeled as a multipole sphere. The blue sphere represents a finite size emitter constituted of three spatially separated but coupled dipoles, to simulate a multipole quantum emitter (QE) with three possible modes. Three little violet balls with green arrows represent these three dipoles with random polarizations.

III. RESULTS AND DISCUSSION

Figure 1 shows atomic force microscopy (AFM) and transmission electron microscopy (TEM) images of a typical QD film doped with AuNPs demonstrating their compact structure. The average surface separation R is obtained by calculating pair-correlation functions of the TEM images of hybrid films. Details of the samples are described in Table I and the Supplemental Material (SM) [36]. To model the experimental data for PL from these hybrid films, theoretical models for both single excitation and repeated excitation [33] were utilized to calculate various parameters like decay rates (Γ) of emitters in a configuration similar to the experimental system. Figure 1(c) illustrates the various regimes and interactions possible in such QE-MNP systems. We can distinguish two regimes of interactions between QEs and AuNPs depending on their separation R. The main outcome of our numerical method involves incorporating finite size of the QEs D_E as well as allowing for renormalization of the emitter decay rates due to coherent energy exchange with AuNPs in the regime of strong coupling. Both these effects seem to become significant when D_E becomes comparable to R and D_E $<$10 nm. When probability of the re-excitation of the emitter by the excited AuNP, i.e., Rabi frequency (Ω) is much smaller than the probability of decay of the excited AuNP (Γ), the weak coupling ($\Omega \ll \Gamma$) approximation will hold [see Fig 1(c)]. Otherwise, in addition to the inhibited dissipation in AuNP, the quantum interference due to superposition of repeated excitations has to be taken into account. Note that the quantum nature and interpretation of the interactions are salient here, rather than quantization of the emitter or the metal [37,38]. Γ_0^r and Γ represent the decay of independent QE and the AuNP. In the weak vacuum-coupling regime, the total radiative and nonradiative parts are a sum of the free

TABLE I. Sample details.

Sample index[a]	R_{C-C} (nm)	R (nm)
A_1C	7.11	1.9
A_2C	7.86	2.65
A_3D	8.12	2.91
A_4D	8.63	3.42
A_5C	8.75	3.54
A_6D	9.5	4.29
A_7C	9.72	4.51
A_8D	10.75	5.54
B_9C	8.93	2.23
Q_4C	11.32	4.58

[a]The table shows the sample indexes of AuNP-doped QD films where A_1C, A_2C, A_5C, A_7C systems are differed by different ligands attached to QDs and AuNPs that leads to nonidentical R values and systems A_3D, A_4D, A_6D, A_8D are prepared by varying density of the particles. Here we have considered Rc-c as the distance between centers of two nanoparticles, whereas R is defined as the separation between the surfaces of those particles. We have observed the maximum efficiency in the system A_5C. The table also contains the sample index referencing QD film (Q_4C). Other reference samples $Q_\alpha C$ differ by various surface separations [36].

space and metallic components as below.

$$\Gamma^r_{\text{total}} = \Gamma^r_0 + \Gamma^r, \Gamma^{nr}_{\text{total}} = \Gamma^{nr}_0 + \Gamma^{nr}, \tag{1}$$

where Γ^r and Γ^{nr} are additional radiative and nonradiative decay rates of emitters due to the presence of metal nanostructure, adding to the total metallic contribution Γ. It is given by the imaginary part of the metal's self-energy contribution Σ, i.e., $\Gamma = -2Im(\Sigma)$; these units reflect a normalization by the reduced Planck's constant as in Eq. (3), describing the real part. This contribution of the nanostructure to self-energy of an emitter at $\mathbf{r_o}$ is given by

$$\Sigma(\omega) = \frac{-2\pi q^2 \omega}{mc^2} \mathbf{e}_o \cdot \mathbf{G}(\mathbf{r_o}, \mathbf{r_o}; \omega) \cdot \mathbf{e}_o, \tag{2}$$

$$\Delta E = \hbar\Omega = 2\hbar|Re(\Sigma)|, \tag{3}$$

where a rotating wave approximation is useful when $\Omega \ll \omega$, and an integral over emission frequencies ω is possible, and q is the oscillating charge, m its mass, and c the speed of light. In the weak vacuum-coupling and strong matter-coupling regime, it was shown that a significant portion of the nonradiative component of the dipole mode of the nanostructure manifests as a radiative component (Γ_{leak}). These modified decay rates of a point dipole emitter can be decomposed in the following manner [33]. Further details of our extended evaluations of the self-interaction dyads $\mathbf{G}$ and the self-energies for finite sized multipole emitters are available in the SM [36].

$$\Gamma_{\text{leak}} = e^{-\frac{\Gamma}{\Omega}} \cdot \Gamma^{nr}_1. \tag{4}$$

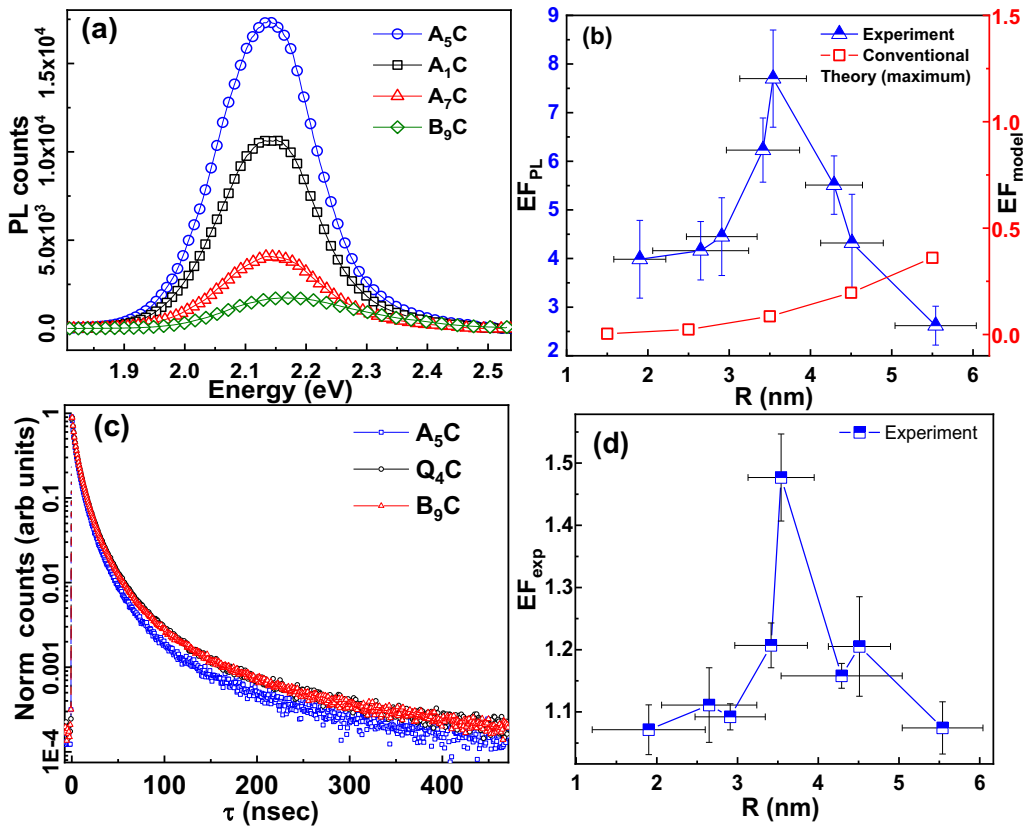

FIG. 2. Steady-state and time-resolved PL data for various AuNP-doped QD films. (a) The individual PL emission spectra for different R. Green curve shows the behavior of the system in presence of larger nanoparticle. (b) The enhancement factor (EF_{PL}) is quantified from the PL measurement as a function of R. (c) Individual decay spectra for different films. (d) Enhancement factor in decay rate (EF_{exp}) is calculated as the ratio of decay rates of AuNP doped QD film to the reference QD film.

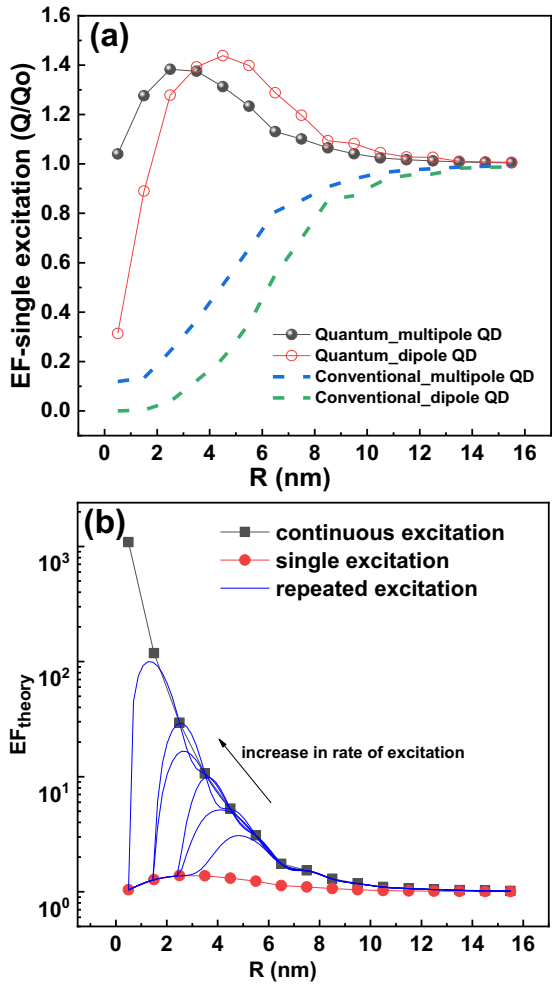

FIG. 3. Results from calculations of QD-AuNP interactions. (a) Predictions of efficiency using different theoretical models for $Q_o = 0.5$. It represents enhancements in emission for a single excitation. (b) Enhancement factors (EF_{theory}) predicted for repeated excitations.

This rate accounts to a vanishing of nonradiative absorption of the dipole mode numbered 1, and its appearance as a stronger radiative mode. The effective decay rates thus become

$$\Gamma^r_{\text{eff}} = \Gamma^r_0 + \Gamma^r + \Gamma_{\text{leak}}, \tag{5}$$

$$\Gamma^{nr}_{\text{eff}} = \Gamma^{nr}_0 + \Gamma^{nr} - \Gamma_{\text{leak}}. \tag{6}$$

In Fig. 2, PL measurements on some of the films are shown clearly demonstrating the large enhancements with respect to reference films containing only the QDs at identical densities (SM, Fig 9). Figure 2(a) also shows PL spectra for films with the same QDs and a similar value of R, as above, but doped with larger size AuNP ($D_M = 8.2$ nm), showing a strong quenching which is similar to the earlier observations [30,39]. This suggests the emergence of a new regime of interactions which is strongly dependent on the size of the AuNPs. In Fig. 2(b), we summarize the observed variation of EF_{PL} with R. The enhancement factor in PL measurement defined as $\text{EF}_{\text{PL}} = \frac{I_{\text{doped}}}{I_{\text{ref}}}$, where I_{doped} and I_{ref} are emitted

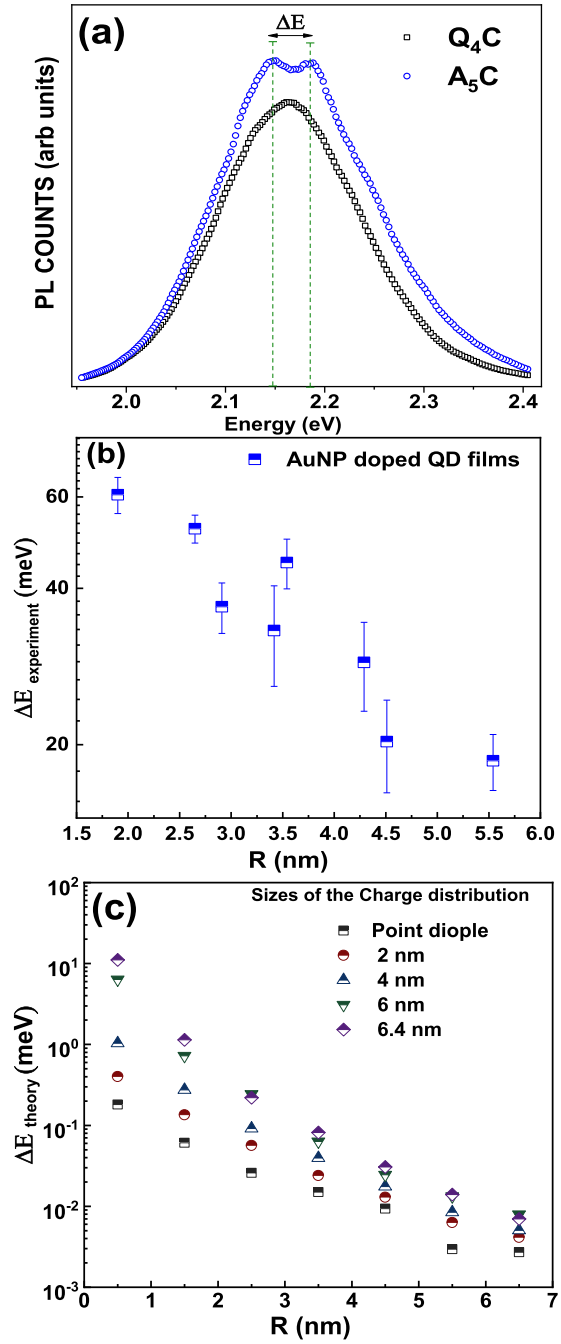

FIG. 4. Strong coupling between QDs and AuNPs. (a) Individual spectra corresponding to reference QD film (Q_4C) and AuNP-doped QD film (A_5C). (b) Energy splitting in PL emission varying with the separation R due to strong coupling among QDs and AuNPs. (c) Theoretically predicted energy shifts for emitting charge distributions of finite sizes; note log scale and actual variations between model predictions at larger separations R are extremely small compared to variations at smaller separations on the left of the figure.

photon counts from the AuNP-based hybrid films and the corresponding reference QD film. It shows a very interesting nonmonotonic variation of EF_{PL} with its maximum at $R = 3.5$ nm but remains >1 within the entire range. The significance of this observed anomalous behavior can be comprehended by comparing this experimental data with predictions

from conventional models of density of optical states that predict a strong quenching in this regime.

A similar behavior is also observed in the measured lifetime of QDs in these films from the time-resolved PL (TRPL) measurements. A weighted decay rate ($\Gamma^{\rm exp}$) was calculated from the average lifetime of QDs in each film by a single excitation using a pulsed laser. The enhancement factor ($\rm EF_{exp}$) is defined as $\rm EF_{exp} = \frac{\Gamma^{exp}_{doped}}{\Gamma^{exp}_{ref}}$, where $\Gamma^{\rm exp}_{\rm doped}$ and $\Gamma^{\rm exp}_{\rm ref}$ are weighted multiexponential fits of the decay of the AuNP-doped hybrid films and the corresponding reference QD films. Results presented in Fig. 2(d), though they do not fully represent the enhancement in the radiative rate, confirm the unexpected nonmonotonic behavior that cannot be explained by the Purcell enhancements (weak coupling) of the extremely small AuNP used in our study, which is almost fully absorbing. Enhancements of photon counts in such pulsed lifetime measurements also allowed us to directly estimate the increase in quantum efficiency, as these experiments represent a single excitation of emitters. Additional experimental results using the TRPL measurements along with the relevant theoretical predictions are presented in the SM. Whereas in the PL spectroscopy experiments using a CW laser excitation [Figs. 2(a) and 2(b)], both the increase in quantum efficiencies and the increase in ground-state population (due to increase of total decay rates), manifest as increased photon counts. While this results in an observed enhancement up to a factor of 8, the quantum efficiencies in turn also increased by a factor of 4, as shown in the SM.

In Fig. 3(b), we highlight this distinction between enhancements due to single and repeated excitations for an example QD with efficiency of 0.5. Different approximations possible in the theoretical evaluations are also shown in Fig. 3(a) and, as mentioned earlier, only the quantum strong-coupling model predicts a nonmonotonic behavior. Classically, weak coupling (Purcell) regime with or without the finite size of QEs completely fails to capture the observed efficiency enhancements in our experiments. The results thus shed light on how the well-established tenets of weak matter-coupling approximation breaks down in the regime of small QE-AuNP separations, R. Note that strong coupling should also result in a clearly observable splitting of the emitted energy when it satisfies the well-known criteria ($\Omega \gg \Gamma$), and weakly observable otherwise.

In Fig. 4(a), we demonstrate this splitting that we observe in the high-resolution PL spectra of a particular film (SM, Fig. 9). Interestingly, we observe a very strong R dependence of the magnitude of this splitting, ΔE. More importantly, Fig. 4(b) shows the observed experimental splitting in AuNP-doped QD films and Fig. 4(c) shows the theoretically predicted values for the point dipole emitter approximation and a finite size multipole emitter with three modes, where both include interactions between QD and AuNP [40].

Note that the average splitting of finite size emitter represents the observed values reasonably well, whereas the splitting evaluated for a point emitter interacting with the AuNP is considerably lower than observed values. It was observed that the two regimes of interactions between QEs and AuNPs can be distinguished depending on their separation R, and the energy splitting ΔE observable. Inclusion of more number of modes in the theoretical model of a finite size emitter is expected to capture experiments even better at shorter separations. Recall that the predicted decay rates and efficiency [in Fig. 3(a)] are not very different for both models, while only the model of finite size emitter predicts the energy-shifts in Fig. 4(b). This also again confirms that while at short distances the strong coupling with nanoparticles is indeed dominant, the finite size of emitters (QDs) results in much larger energy shifts that are observable even in the inhomogeneously broadened PL spectra.

IV. CONCLUSION

In summary, our combined experimental and theoretical studies of compact QD films doped with ultrasmall fully absorbing AuNPs at very small QD-AuNP separations demonstrates the emergence of a new photonic regime of large emission enhancement. This regime goes beyond the well-established Purcell regime and can only be explained by invoking strong-coupling effects and the finite size of the emitter. The fact that incorporation of these nonclassical or quantum interactions which become increasingly relevant at very small QE-AuNP separations leads to the explanation of our experimental results, suggests the emergence and importance of quantum plasmonics in treating emitter-matter interactions at the nanoscale. These results can have a significant impact on future photonics and display devices and provide new directions in fundamental research in nanophotonics, quantum photonics, and information processing.

ACKNOWLEDGMENTS

We acknowledge the Department of Science and Technology (Nanomission) and SERB India for the financial support and the Advanced Facility for Microscopy and Microanalysis (AFMM) Indian Institute of Science, Bangalore, for the access to TEM measurements. R.D. acknowledges DST for financial support.

[1] H. A. Atwater and A. Polman, Nat. Mater. **9**, 205 (2010).

[2] A. Kiraz, M. Atatüre, and A. Imamoğlu, Phys. Rev. A **69**, 032305 (2004).

[3] F. Liu, A. J. Brash, J. O'Hara, L. M. Martins, C. L. Phillips, R. J. Coles, B. Royall, E. Clarke, C. Bentham, N. Prtljaga *et al.*, Nat. Nanotechnol. **13**, 835 (2018).

[4] I. L. Medintz, H. T. Uyeda, E. R. Goldman, and H. Mattoussi, Nat. Mater. **4**, 435 (2005).

[5] S. Fafard, K. Hinzer, S. Raymond, M. Dion, J. McCaffrey, Y. Feng, and S. Charbonneau, Science **274**, 1350 (1996).

[6] R. F. Oulton, V. J. Sorger, T. Zentgraf, R.-M. Ma, C. Gladden, L. Dai, G. Bartal, and X. Zhang, Nature **461**, 629 (2009).

[7] M. V. Kovalenko, Nat. Nanotechnol. **10**, 994 (2015).
[8] J. Tang and E. H. Sargent, Adv. Mater. **23**, 12 (2011).
[9] D. V. Talapin and C. B. Murray, Science **310**, 86 (2005).
[10] C. R. Kagan, C. B. Murray, M. Nirmal, and M. G. Bawendi, Phys. Rev. Lett. **76**, 1517 (1996).
[11] C. R. Kagan and C. B. Murray, Nat. Nanotechnol. **10**, 1013 (2015).
[12] W.-L. Ong, S. M. Rupich, D. V. Talapin, A. J. McGaughey, and J. A. Malen, Nat. Mater. **12**, 410 (2013).
[13] D. J. Bergman and M. I. Stockman, Phys. Rev. Lett. **90**, 027402 (2003).
[14] D. Ratchford, F. Shafiei, S. Kim, S. K. Gray, and X. Li, Nano Lett. **11**, 1049 (2011).
[15] F. Intravaia and K. Busch, Phys. Rev. A **91**, 053836 (2015).
[16] E. M. Purcell, H. C. Torrey, and R. V. Pound, Phys. Rev. **69**, 37 (1946).
[17] E. M. Purcell, in *Confined Electrons and Photons* (Springer, Berlin, 1995), pp. 839–839.
[18] K. Drexhage, J. Lumin. **1-2**, 693 (1970).
[19] P. T. Worthing, R. M. Amos, and W. L. Barnes, Phys. Rev. A **59**, 865 (1999).
[20] M. Pelton, Nat. Photonics **9**, 427 (2015).
[21] N. J. Halas, S. Lal, W.-S. Chang, S. Link, and P. Nordlander, Chem. Rev. **111**, 3913 (2011).
[22] M. Haridas, J. Basu, D. Gosztola, and G. Wiederrecht, Appl. Phys. Lett. **97**, 083307 (2010).
[23] M. Haridas, L. Tripathi, and J. Basu, Appl. Phys. Lett. **98**, 063305 (2011).
[24] M. Praveena, A. Mukherjee, M. Venkatapathi, and J. K. Basu, Phys. Rev. B **92**, 235403 (2015).
[25] M. Haridas, J. Basu, A. Tiwari, and M. Venkatapathi, J. Appl. Phys. **114**, 064305 (2013).
[26] K. A. Kang, J. Wang, J. B. Jasinski, and S. Achilefu, J. Nanobiotechnol. **9**, 16 (2011).
[27] G. Schneider, G. Decher, N. Nerambourg, R. Praho, M. H. V. Werts, and M. Blanchard-Desce, Nano Lett. **6**, 530 (2006).
[28] K. Nasiri Avanaki, W. Ding, and G. C. Schatz, J. Phys. Chem. C **122**, 29445 (2018).
[29] D. Cheng and Q.-H. Xu, Chem. Commun. 248 (2007).
[30] E. Dulkeith, M. Ringler, T. Klar, J. Feldmann, A. Munoz Javier, and W. Parak, Nano Lett. **5**, 585 (2005).
[31] S. Kühn, U. Håkanson, L. Rogobete, and V. Sandoghdar, Phys. Rev. Lett. **97**, 017402 (2006).
[32] M. Venkatapathi, J. Quant. Spectrosc. Radiat. Transfer **113**, 1705 (2012).
[33] K. Jain and M. Venkatapathi, Phys. Rev. Appl. **11**, 054002 (2019).
[34] P. Anger, P. Bharadwaj, and L. Novotny, Phys. Rev. Lett. **96**, 113002 (2006).
[35] R. Thomas, A. Thomas, S. Pullanchery, L. Joseph, S. M. Somasundaran, R. S. Swathi, S. K. Gray, and K. G. Thomas, ACS Nano **12**, 402 (2018).
[36] See Supplemental Material at http://link.aps.org/supplemental/10.1103/PhysRevB.100.155413 for more details on the preparation of samples, analysis, and related additional figures.
[37] A. Trügler and U. Hohenester, Phys. Rev. B **77**, 115403 (2008).
[38] T. Hümmer, F. J. García-Vidal, L. Martín-Moreno, and D. Zueco, Phys. Rev. B **87**, 115419 (2013).
[39] G. Zengin, M. Wersäll, S. Nilsson, T. J. Antosiewicz, M. Käll, and T. Shegai, Phys. Rev. Lett. **114**, 157401 (2015).
[40] J. Bellessa, C. Symonds, K. Vynck, A. Lemaitre, A. Brioude, L. Beaur, J. C. Plenet, P. Viste, D. Felbacq, E. Cambril, and P. Valvin, Phys. Rev. B **80**, 033303 (2009).